THE ASTROPHYSICAL JOURNAL, 445:L153–L156, 1995 June 1

THE DISCOVERY OF A JETLIKE FEATURE FROM THE MASSIVE STAR HERSCHEL 36[1]

B. STECKLUM AND T. HENNING
MPG Arbeitsgrupper Staub in Sternentstehungsgebieten, Schillergäßchen 3, D-07745 Jena, Germany;
pbs@physik.uni-jena.de, henning@fred.astro.uni-jena.de

A. ECKART
Max-Planck-Institut für Extraterrestrische Physik, Gießenbachstraße 1, D-85748 Garching, Germany;
eckart@mpa-garching.mpg.de

R. R. HOWELL
Department of Physics and Astronomy, University of Wyoming, Laramie, WY 82071;
rhowell@uwyo.edu

AND

M. G. HOARE
Max-Planck-Institut für Astronomie, Königstuhl 17, D-69117 Heidelberg, Germany;
mgh@mpia-hd.mpg.de

Received 1994 December 14; accepted 1995 March 21

ABSTRACT

The O7 V star Herschel 36 has been studied in the near-infrared by ground-based high-resolution techniques. These observations and image restoration of *Hubble Space Telescope* planetary camera Hα and [S II] images led to the detection of a jetlike feature. The interpretation of that feature as a jet is discussed in relation to a circumstellar disk for which evidence exists.

Subject headings: circumstellar matter — ISM: jets and outflows — stars: imaging

1. INTRODUCTION

The star Herschel 36 (Her 36, $\alpha_{1950} = 18^h00^m36^s.3$, $\delta_{1950} = -24°22'53''$) located west of the Hourglass Nebula in M8 has been classified as an O7 V star (Woolf 1961). The brightness of Her 36 in the infrared (Woolf et al. 1973) indicates the presence of circumstellar dust with an unresolved (2″) core at 10 μm, a pronounced absorption feature at this wavelength attributed to silicates, and a strong mid-infrared excess due to emission from polycyclic aromatic hydrocarbons (PAHs). The detection of H_2CO at 6 cm wavelength (Zuckerman et al. 1970) and of millimeter HCN emission (Giguere, Snyder, & Buhl 1973) toward Her 36 revealed the presence of a large molecular cloud. A comprehensive analysis (Lada et al. 1976) of the CO, radio continuum, and optical data indicated that Her 36 is the most likely ionizing source for most of the M8 region. One of the peaks of the CO emission coincides with the star. Shortly after this finding, another strong infrared source associated with intense CO emission, M8E, was discovered 19′ east of Her 36 (Walker & Price 1975; Wright et al. 1977), which later attracted much of the attention devoted to the investigation of the M8 region (see, e.g., Henning et al. 1991).

Far-infrared observations at 2′ resolution by Lightfoot et al. (1984) showed the distribution of the 23–80 μm flux peaking on Her 36 and elongated in the NE-SW direction. From these observations, the presence of a large disk has been suggested, with an orientation of the polar axis about 45°.

Her 36 served as a preferred target in investigations of interstellar extinction and polarization. The extinction curve toward Her 36 (Hecht et al. 1982) is similar to those in other dusty regions, e.g., ρ Oph and Orion. A ratio $R = 5.6$ of total to selective extinction toward Her 36 is indicative of dust grains larger than in the interstellar medium. Furthermore, the absence of a rise in the normalized extinction at wavelengths less than 1800 Å implies that smaller particles are absent.

The integrated polarization of Her 36 drops from 6.5% in the V band (McCall, Richer, & Visvanathan 1990) to about 1% in the L' band (Martin et al. 1992). There is evidence for a change of the orientation of the electric vector with wavelength (Jones 1990; McCall et al. 1990), which suggests a circumstellar component of the polarization in the infrared. The orientation of most of the polarization vectors available in the literature is in the range 40°–90°. The radio continuum emission of Her 36 at 6 cm wavelength has been mapped with the VLA at a resolution of 7″.4 × 3″.2 (Woodward et al. 1986). The distribution of the radio emission mainly covers the northern part of the Hourglass and extends to the west including Her 36. The maximum of the 6 cm radiation according to these observations is about 8″ east of Her 36. More detailed investigations using the VLA at higher resolution revealed the ultracompact H II (UCHII) region G5.97 − 1.17 of core-halo morphology at the position 1″.7 south and 2″.5 east of Her 36 (Wood & Churchwell 1989). The far-infrared and radio luminosities of the UCHII region imply the presence of a star of spectral type earlier than B0. Water maser emission toward the UCHII has been detected (Wood & Churchwell 1989).

Near-infrared imaging (Woodward et al. 1990) led to the suggestion that Her 36 and a candidate pre–main-sequence object (KS1) located 3″.4 north and 0″.4 east of Her 36 may be part of a Trapezium-like stellar cluster.

2. OBSERVATIONS

First evidence for the presence of an extended structure around Her 36 has been obtained by observing a lunar occultation using the 2.3 m WIRO telescope on 1992 May 19. The reappearance was measured in the L' band at a time resolution of 2 ms. The light curve shows no diffraction fringes but a gradual increase of the signal typical for the case of

[1] Based on observations collected at the European Southern Observatory, La Silla, Chile.

geometric obscuration of an extended object (Stecklum et al. 1994a). From this observation, an FWHM of the extended structure of 0".25 has been derived. However, since lunar occultations only yield the one-dimensional brightness distribution of the source (perpendicular to orientation of the lunar limb), no conclusion could be drawn on the spatial distribution of this extended emission. Therefore, we subsequently carried out *K*-band speckle imaging using the SHARP camera (Hofmann et al. 1993) at the ESO NTT telescope. This yielded a nearly diffraction-limited image (0".2 resolution) of a 6".4 × 6".4 region around Her 36 (Stecklum et al. 1994b). This image shows a star at 0".71 distance southwest of Her 36 and a more complex structure at $\lesssim$0".6 distance east to southeast of Her 36.

In order to investigate the immediate environment of Her 36 in more detail and to obtain information on the colors of the newly detected sources in this region, we performed imaging with adaptive optics using ESO's ComeOn+ (Rousset et al. 1994) equipped with SHARP 2 at ESO's 3.6 m telescope. The observations were carried out in the *H* and *K* bands on 1994 March 29 and covered a field of 18".8 × 14".6 around Her 36. The total integration times in the *H* and *K* bands were 500 s and 750 s, respectively. As in the previous speckle observations, the nearby star Sgr 9 served as reference for the point spread function (PSF). The application of the Richardson-Lucy (RL; Lucy 1974) and maximum entropy (ME; Agmon, Alhassid, & Levine 1979) deconvolution algorithms for the restoration of the adaptive optics images yielded a diffraction-limited resolution (0".15) in the *K* band.

The M8 region was observed by the *Hubble Space Telescope* (*HST*) on 1993 October 2 using the planetary camera (PC). Both the 200 s exposure in Hα light (W1DA0201P) and the 600 s exposure in [S II] (W1DA0202P) covered Her 36. On the second image, Her 36 is overexposed. Image restoration for the Hα exposure was carried out using the PSF created by TinyTim (Krist 1994) appropriate for the exposure parameters. For this purpose, the algorithms mentioned above have again been employed.

The spherical aberration of the *HST* PC before the repair enables the restoration of the [S II] image in the saturated part (Hollis, Dorband, & Yusef-Zadeh 1992). This relies on the fact that the light from the wings of the PSF which falls outside the saturated region permits statistical inference. The morphological detail in the area of saturation has been restored by the ME algorithm proposed by Hollis et al. (1992). In order to avoid effects due to nonlinearity of the detector, image levels larger than 60% of the saturation level has been clipped. The PSF for the [S II] image was also constructed using TinyTim (Krist 1994).

During one commissioning run of IRCAM3 at UKIRT, shift-and-add images of Her 36 were obtained at a resolution of 0".15 pixel^{-1} in the *H*, *K*, and narrow *L* (nbL) bands.

3. RESULTS

The *L'*-band light curve of the occultation is shown in Figure 1. The data have been rebinned to 80 ms time resolution equivalent to an angular sampling of 0".026 in order to increase the signal-to-noise ratio, which is about 14 in the displayed graph. There is a secondary event in the light curve about 7 s after the reappearance of Her 36 which is caused by the source KS1. This object is actually a binary star with a very red northern component, which will be discussed in a forthcoming paper (Stecklum et al. 1995).

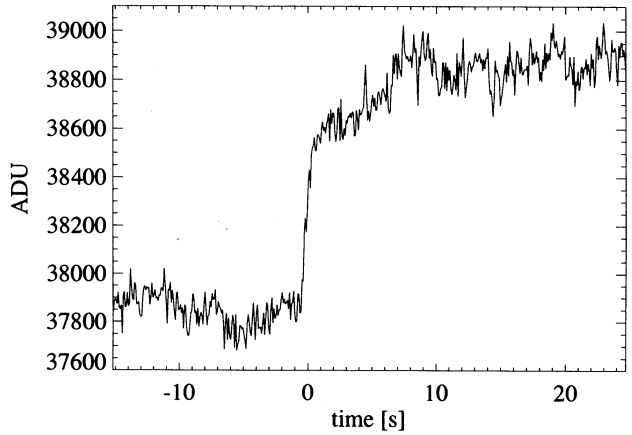

FIG. 1.—Light curve of the reappearance of Her 36 at 80 ms time resolution (equivalent to 0".026 per sample).

The light curve has been deconvolved with the theoretical diffraction pattern using an ME algorithm based on the approach of Frieden (1978). The algorithm takes into account all corresponding observational conditions (integration time, aperture size, bandpass of the telescope) and outputs the smoothest object profile consistent with the noise statistics. The strip brightness distribution in the *L'* band for a position angle of 57°.2 is shown as the dash-dotted line in Figure 2. Due to the total absence of diffraction fringes, the change of the angular scale caused by the local lunar limb slope could not be determined.

From the adaptive optics *K*-band image, the strip brightness distribution has been computed for the lunar limb orientation valid for the observed occultation. This profile is displayed as a solid line in Figure 2.

Figure 3 contains the *HST*-PC Hα image in logarithmic gray scale with intensities as small as 10^{-3} of the normalized peak flux. The overlain contour lines represent the intensity distribution of the adaptive optics *K* image. The lowest level is at 0.0512 Jy arcsec^{-2} and the contours increase by a factor of 2.5. The dotted line illustrates the orientation of the lunar limb

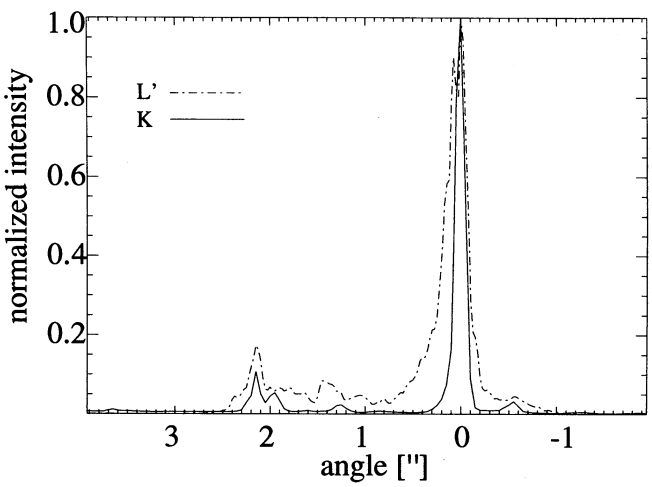

FIG. 2.—Strip brightness distribution of Her 36 and nearby objects. Dash-dotted line is the result of the deconvolution of the occultation light curve. Solid line marks the brightness profile which has been constructed from the adaptive optics imaging results. Both curves have been normalized to peak value unity.

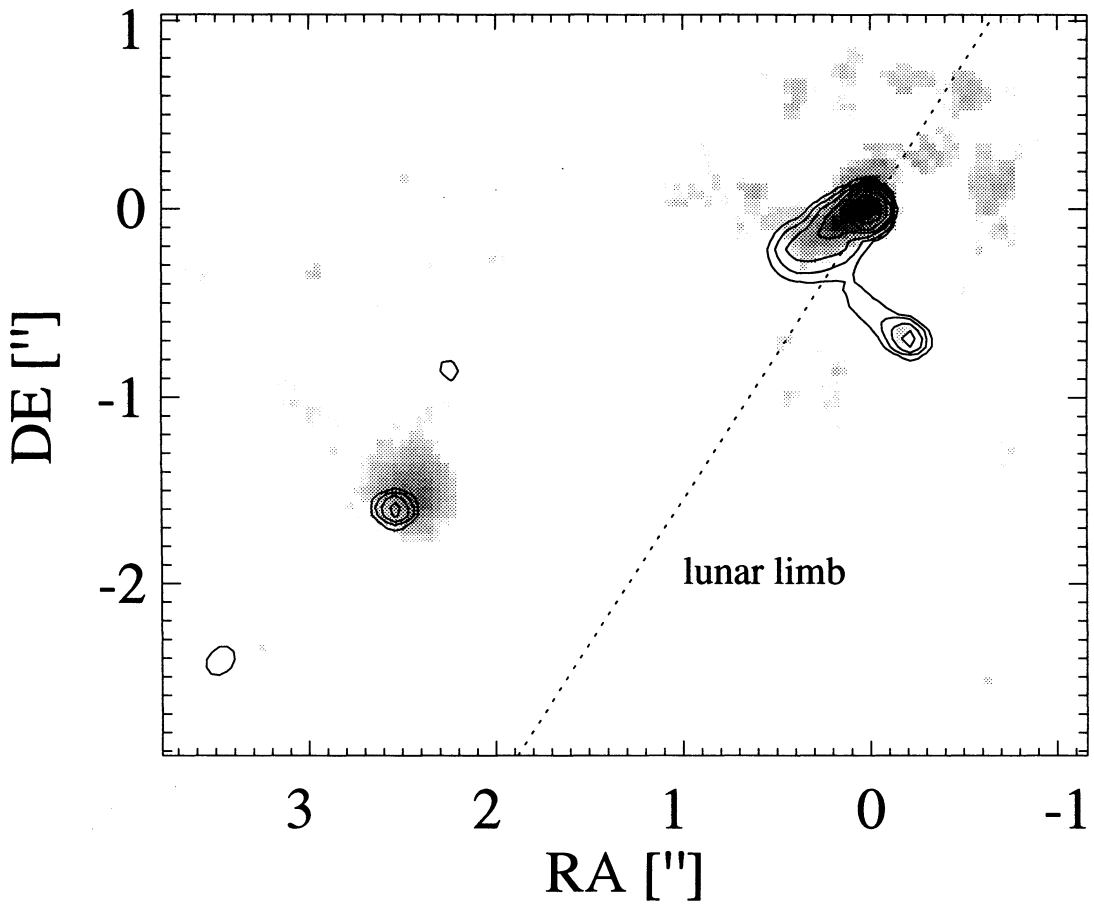

FIG. 3.—*HST*-PC Hα image of Her 36 and its jet. The *K*-band intensity contours are superposed. Dotted line illustrates the lunar limb orientation during the reappearance.

during the occultation. The image shows the elongated structure emerging from Her 36 with an extent of about 0".6 in the *K* band. Since it has a jetlike appearance, we will refer to it as "jet" in the following. On the *H*-band image, no evidence for the jet has been found.

The position angle of the jet is ~124°. It points to the UCHII region, which is unresolved in the near-infrared but resolved in Hα. There is a small displacement between the peak emission of the UCHII region in the *K* and Hα images, respectively.

There are some artifacts in the restored Hα image which result from a slight mismatch of the TinyTim PSF with the actual PSF. The recovered jet structure also appears if a star from the second exposure serves as a point source reference. The bridge between Her 36 and the southwest companion at the lowest contour level of the *K*-band intensity distribution is probably a spurious feature from the RL deconvolution. The restored [S II] image contains the recovered stellar brightness peak and a knot of emission in 0".2 distance at the position angle of the jet.

The small peaks of the brightness profiles (see Fig. 2) at −0".6 distance from Her 36 are caused by the southwest companion. The broad wings of Her 36 at positive angular distance are due to the jet which extends in the *L'* band about twice the distance compared to *K*. The peak at about 1".3 distance is caused by the UCHII region. At about 2" distance, there are two maxima in the *K*-band brightness profile caused by the binary KS1. The increased flux of the northern component of the binary in the *L'*-band profile compared to *K* implies that it is a very red object. This has been confirmed by the nbL imaging with IRCAM3.

From both occultation observations and high-resolution imaging, no evidence has been found for a counterjet extending to the opposite direction.

4. DISCUSSION

The identification of the observed structure close to Her 36 as a jet is based merely on its morphology, since spectroscopy at the angular resolution similar to that of the presented imaging is not available yet. Imaging spectroscopy in the *K* band at a pixel scale of 0".5 shows the emission caused by the UCHII region (Stecklum et al. 1995). At this angular resolution, we were not able to find spectroscopic evidence for the jet.

If the jet interpretation is correct, it can be expected that the observed flux in the *K* and *L'* bands is due to emission lines at 2.17 μm (Brγ) and 4.05 μm (Brα) with no contribution from an underlying continuum. From the extent of the jet in the *L'* strip brightness profile and the difference in position angles between the tangent to the lunar limb and the jet direction (which amounts to 23°.2), we conclude that the jet possibly extends to about 1".5 in the *L'* band. The deconvolved nbL image does not show this structure because the Brα line is not covered by the nbL filter.

There seems to be a condensation in the adaptive optics *K*-band image halfway along the jet which coincides with the

[S II] knot. This feature is slightly south of object 6 of our previous *K*-band speckle image (Stecklum et al. 1994b). We note that there are some differences in the morphology of the structures around Her 36 between the adaptive optics and speckle *K*-band images. Further investigations have to show whether this reflects actual mass motion or is merely due to mismatch of the PSFs used in the deconvolution procedures.

At the distance of M8 of 1.5 kpc (Georgelin & Georgelin 1976), the jet can be traced up to 800 AU in Hα light, up to 950 AU in the *K* band, and up to 2000 AU in the *L'* band. The orientation of the jet is approximately perpendicular to the elongated dust structure seen in the far-infrared by Lightfoot et al. (1984). Its relation to a circumstellar disk cannot be fully explored since the resolution of the available dust-continuum and molecular-line maps is not sufficient.

Jets are one of several outflow phenomena associated with young stars, all of which are probably the result of stellar winds interacting with the surrounding medium. The collimation of stellar winds by the action of circumstellar disks is one possibility to explain the confinement of jets and molecular outflows. There are several arguments which suggest the presence of such a disk around Her 36. First, our observations do not show a counterjet that will be hidden if the disk is inclined so that the western part of the disk shadows this jet. Jets of low- and medium-mass stars are usually accompanied by molecular outflows. While there is no observation of such an outflow in the case of Her 36, the CO emission near Her 36 appears to be blueshifted with respect to the rest of the cloud (Lada et al. 1976). The distribution of the 11.1 μm emisson at the resolution of 4".5 peaks on Her 36 and extends from about 5" west of the star to about 14" east of the Hourglass Nebula. While the emission decreases rather smoothly to the east, the drop at the western border is very pronounced (Dyck 1977). This emission might be caused by heating of the disk surface by back-scattered photons from the dusty environment. We note, however, that at these wavelengths the northern component of KS1 will contribute a considerable fraction to the total flux.

Most jet sources are highly polarized, with the electric polarization vector approximately perpendicular to the jet orientation. While there is some scatter in the position angles of the polarization vectors for Her 36 at different wavelengths (which might reflect a wavelength dependence), the values are consistent with the jet marking the symmetry axis of the disk. The unusual extinction curve toward Her 36 suggests the presence of dust grains larger than those in the diffuse interstellar medium. This may be explained by dust particles which grew in the circumstellar disk by coagulation and agglomeration. Her 36 may be the first example of a visible, young massive star more evolved than the exciting stars of Becklin-Neugebauer objects and UCHII regions which still shows signposts of star formation. The study of this object might give new insights for the problems of circumstellar disk evolution and jet formation of massive stars.

B. S. acknowledges support from grant DFG Ste 605-2. Thanks are due to the SHARP and ComeOn+ teams, whose assistance during the speckle and adaptive optics runs was essential for obtaining the described results.

REFERENCES

Agmon, N., Alhassid, Y., & Levine, R. D. 1979, J. Comput. Phys. 30, 250
Dyck, H. M. 1977, AJ, 82, 129
Frieden, B. R. 1978, J. Opt. Soc. Am., 68, 93
Georgelin, Y. M., & Georgelin, Y. P. 1976, A&A, 49, 57
Giguere, P. T. Snyder, L. E., & Buhl, D. 1973, ApJ, 182, L11
Hecht, J., Helfer, H. L., Wolf, J., Donn, B., & Pipher, J. L. 1982, ApJ, 263, L39
Henning, T., Gürtler, J., Krügel, E., & Chini, R. 1991, A&A, 252, 801
Hofmann, R., Blietz, P., Duhoux, P., Eckart, A., Krabbe, A., & Rotacuic, V. 1993, in Progress in Telescope and Instrumentation Technologies, ed. M. H. Ulrich (ESO Rept. 42), 617
Hollis, J. M., Dorband, J. E., & Yusef-Zadeh, F. 1992, ApJ, 386, 293
Jones, T. J. 1990, AJ, 99, 1894
Krist, J. 1994, TinyTim Users Manual, Version 4.0
Lada, C. J., Gull, T. R., Gottlieb, C. A., & Gottlieb, E. W. 1976, ApJ, 203, 159
Lightfoot, J. F., Deighton, D. W., Furniss, I., Glencross, W. M., Hirst, C. J., Jennings, R. E., & Poulter, G. 1984, MNRAS, 208, 197
Lucy, L. B. 1974, AJ, 79, 745
Martin, P. G., Adamson, A. J., Whittet, D. C. B., Hough, J. H., Bailey, J. A., Kim, S.-H., Sato, S., Tamura, M., & Yamashita, T. 1992, ApJ, 392, 691
McCall, M. L., Richer, M. G., & Visvanathan, N. 1990, ApJ, 357, 502
Rousset, F., et al. 1994, Proc. SPIE, 2201, 1088
Stecklum, B., Henning, T., Eckart, A., Krabbe, A., Hoare, M. G., & Puxley, P. 1995, in preparation
Stecklum, B., Henning, Th., Eckart, A., & Hofmann, R. 1994b, NIR High-Resolution Imaging of Young Stars, Infrared Phys., 35, 487
Stecklum, B., Howell, R. R., Eckart, A., & Richichi, A. 1994a, in IAU Symp. 158, Very High Angular Resolution Imaging, ed. J. G. Robertson & W. J. Tango (Dordrecht: Kluwer), 364
Walker, R. G., & Price, S. D. 1975, AFCRL Infrared Sky Survey (AFCRL-TR-75-0373)
Wood, D. O. S., & Churchwell, E. 1989, ApJS, 69, 831
Woodward, C. E., Pipher, J. L., Helfer, H. L., & Forrest, W. J. 1990, ApJ, 365, 252
Woodward, C. E., et al. 1986, AJ, 91, 870
Woolf, N. J. 1961, PASP, 73, 206
Woolf, N. J., Gillet, F. C., Merrill, K. M., Becklin, E. E., & Neugebauer, G. 1973, ApJ, 179, L111
Wright, E. L., Lada, C. J., Fazio, G. G., & Kleinmann, D. E. 1977, AJ, 82, 132
Zuckerman, B., Buhl, D., Palmer, P., & Snyder, L. E. 1970, ApJ, 160, 485